Ashlin, Samuel John; Sannasiraj, Sannasi Annamalaisamy; Sundar, Vallam

Performance of an Oscillating Water Column Device with Different Bottom Profiles Subjected to Random Waves

ICHE 2014, Hamburg - Lehfeldt & Kopmann (eds) - © 2014 Bundesanstalt für Wasserbau ISBN 978-3-939230-32-8

Performance of an Oscillating Water Column Device with Different Bottom Profiles Subjected to Random Waves

S. John Ashlin, S.A. Sannasiraj & V. Sundar
Department of Ocean Engineering, Indian Institute of Technology Madras, Chennai, India.

ABSTRACT: The effect of the shape inside the chamber of an oscillating water column (OWC), integrated to a bottom fixed breakwater on its efficiency is considered. For this study, an oscillating column device with four different bottom profiles (flat bottom, bottom with a slope of 1:1 and 1:1.5 and circular arc bottom of radius 300mm) were taken up for investigation. The models were installed in a water depth, d of 0.5m and subjected to random waves with peak period varying from 1s to 3s thus, covering steepness, H_{m0}/L_p ranging between 0.014 and 0.062 and relative water depth, d/L_p from 0.078 to 0.330. For each of the four models as stated above, exposed to random waves, the variations of its hydrodynamic efficiency, wave amplification and other spectral characteristics like spectral moment, and are studied and the results are presented as a function of relative water depth for the range of H_{m0}/d from 0.1010 to 0.1564. From the hydrodynamic efficiency, the circular arc bottom profile is found to have maximum hydrodynamic efficiency compared to the other bottom profiles considered. The OWC gives a better performance in the low frequency than in high frequency.

Keywords: Random waves, Wave amplification, Hydrodynamic efficiency, Wave energy, OWC

1 INTRODUCTION

Of the different sources from tides, current, wind and waves, there has been tremendous progress in research and development of wave energy and offshore wind energy devices/concepts as they are considered to be clean energy. In the case of wave energy conversion, an interface device, Wave Energy Converter (WEC) is needed to convert energy in the waves to mechanical energy prior to its conversion into electric energy. Numerous concepts have been proposed; with power rating ranging from a few Watts to mega Watts. An OWC device consists of a vertical caisson having an opening on the wave beaten side and an air chamber above the water surface. The dynamic pressure under the ocean wave near the opening causes flow oscillations inside the air chamber. The rise of water inside the chamber compresses the air to develop pneumatic power. Thus, it can cause air flow at high velocity through a duct that can rotate a turbine on its path. In the second phase, as the water falls down creates a vacuum in the chamber which absorbs air through the duct. Thus, a bi-axial air turbine placed in the duct can convert the cyclic pneumatic power into unidirectional movement of turbine for generating electricity. Malmo and Reitan (1985) observed that the natural frequency of an OWC system mainly depends on the front lip depth. McIver and Evans (1988) showed that the response of OWC system depends on magnitude of the dynamic pressure and its excitation period. Zheng et al., (1989) found out that flared harbour walls enhanced the efficiency compared to the rectangular walls. Front wall submergence (a), chamber length (b) and water depth (h) were considered to be key parameters by Evans and Porter (1995). It was observed that for smaller values of b/h, the fluid behaves like a rigid body inside the OWC chamber. It was also observed that for larger values of a/h, the efficiency band was narrowing. The lip wall thickness was not considered in the study. Thiruvenkatasamy and Neelamani (1997) by varying center spacing (S) between adjacent units have reported that the optimized spacing ratio (S/b) is 3. It was also observed that the increase in wave steepness (H/L) caused a decrease in efficiency and for a/A (ratio of air hole area (a) to plan area (A)) greater than 0.81, there was a significant reduction in energy absorption capacity of the device. Thomas et al., (2007) observed through their experimental study that the thickness of the front wall did not have any influence on energy conversion capacity of the device. Sundar et al., (2010) presented a comprehensive review on

novel approaches that can utilize the wave energy converters as part of coastal defense systems, breakwaters for the formation of harbors as well as for offshore applications. Zhang et al., (2012) found that the performance of OWC on efficiency produced a banded pattern centered with a resonant peak. This indicates the development of phase difference between the dynamic excitation pressure and the corresponding air pressure being developed. Wilbert et al., (2013) have taken the parameters such as bottom opening of the energy converter (o) and depth of water inside the energy converter (d_i) and, found that energy conversion capacity of OWC was found to be increasing with O/d_i. It reached a maximum efficiency of 94% closer to the resonant frequency for O/d_i=0.80. At the same time, with an increase in opening depth, the peak efficiency shifts towards the higher frequency.

2 EXPERIMENTAL SETUP

The present paper mainly focuses on the performance of OWC model in random wave field. For this purpose, an experimental study on four different bottom configurations, viz., flat, circular arc of radius 300mm, a slope of 1:1 and 1:1.5 were considered for the tests. Experiments were conducted in a wave flume 72.5m long and 2 m wide. One end of the flume installed with a computer controlled wave maker is capable of generating random waves another end with wave absorber. A parabolic perforated beach wave absorber on the other end is capable of absorbing energy in the generated waves up to about 90%. The wave flume was longitudinally divided into four compartments to facilitate simultaneous testing of the four models as mentioned above. The test set-up was located at a distance of 45m from the wave maker. The models were made of 12mm thick acrylic sheet, each of which of dimensions 471 x 300 mm in plan with a height of 900mm. The depth of the front wall of each of the model was 600mm from the top and front wall opening was 300mm. The longitudinal view of the present experimental setup is shown in Figure 1.

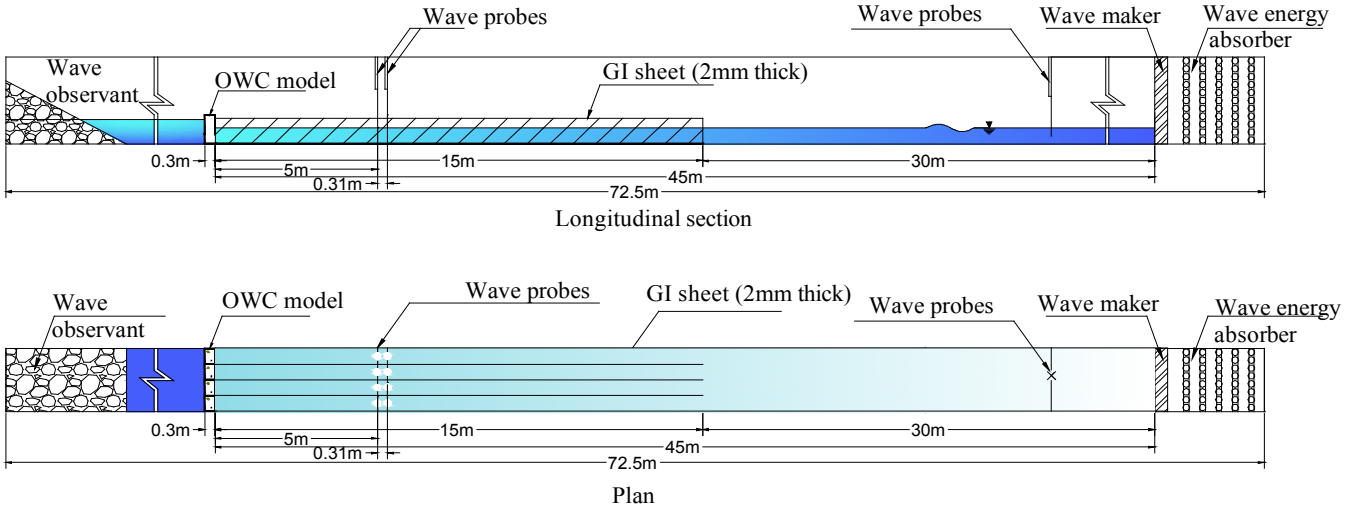

Figure 1. Wave flume and test setup.

The arrangements and dimensional details of the models in plan and sectional elevation of the model with circular arc bottom of radius 300mm are shown in Figure 2. For each of the models, an air vent was maintained as 0.68% of the plan area of the device. Three wave probes, one at a distance of 7m from the wave maker and the other two at 5m and 5.3m from the model, inside each of the four longitudinal sections, were used to measure the wave elevations. A probe to measure the water level rise and fall on the rear wall of the air chamber, (run-up, R_u) pressure transducers one facing the waves (P_{fout}) and another to register the pressure variations on the front wall on its rear side (P_{fin}) were fixed to each of the four models. The air pressure inside the chamber of each of the four models was measured with a pressure sensor on top (P_{air}). In essence, three pressure signals, one run-up and two wave probes for deriving the reflection coefficient for each of the four models, plus one incident water wave elevation, thus, in total 25 channels of signatures were simultaneously acquired with a sampling interval of 0.05s for further processing of the measurements.

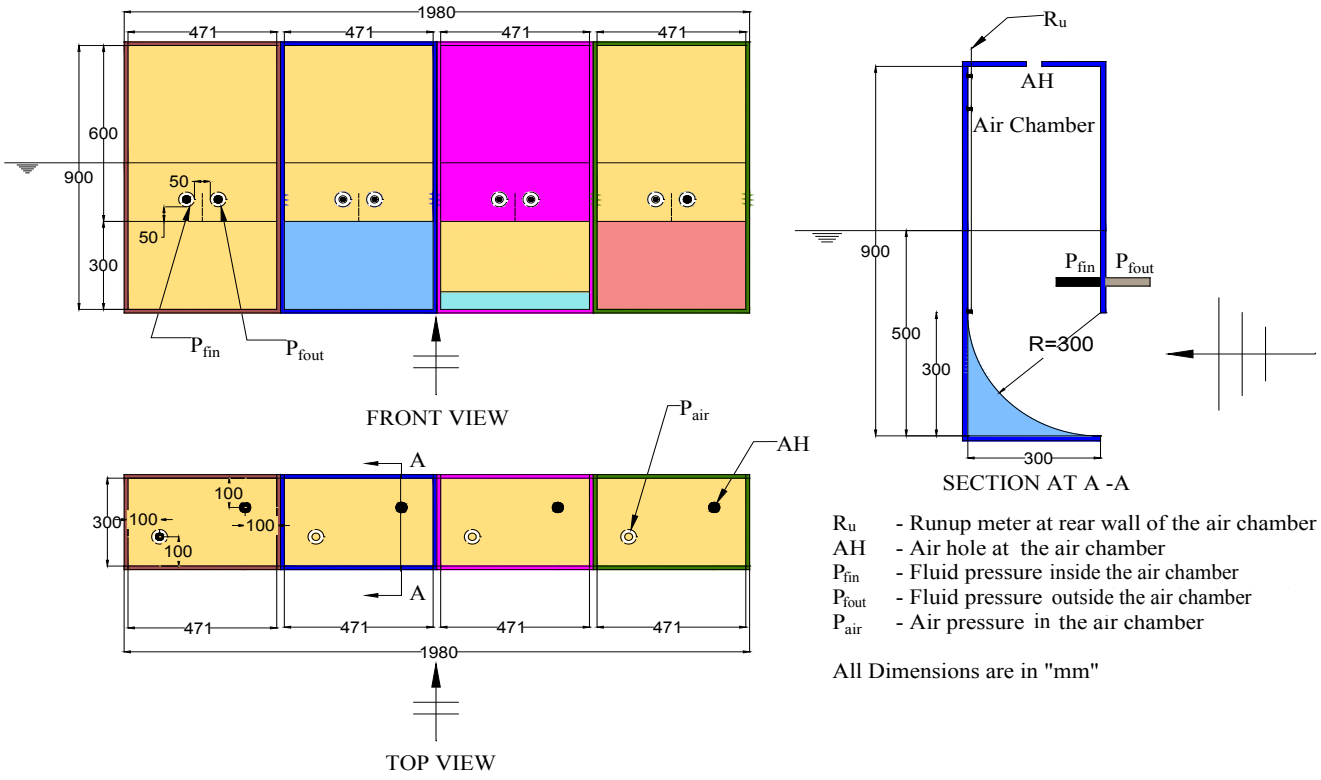

Figure 2. Details of OWC models tested.

In the experimental work the performance of each of the OWC device with the different bottom configuration were measured in a water depth, d of 0.5m for a wide range of wave characteristics, with frequencies ranging between 0.33Hz and 1.0Hz such that wave steepness, H_{m0}/L_p ranged from 0.014 to 0.062 and relative water depth, d/L_p ranged from 0.078 to 0.330, where 'H_{m0}' and 'L_p' are the Spectral estimate of the significant wave height and wave length corresponding to peak period respectively. The model units with the cables and connectors exposed the waves are shown in Figure 3.

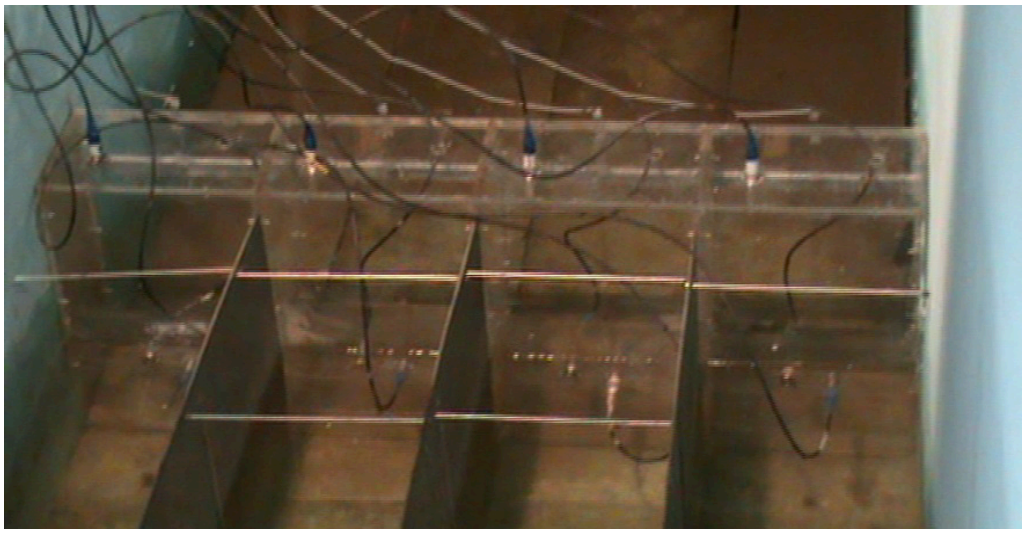

Figure 3. Setup of OWC in wave flume.

3 RESULTS AND DISCUSSION

3.1 *General*

For the laboratory studies the random waves described by Pierson – Moskowitz (PM) spectrum adopted and is given below in Equation 1.

$$S(f) = \frac{5H_S^2}{16 f_P}\left(\frac{f_P}{f}\right)^2 \exp\left[-\frac{5}{4}\left(\frac{f_p}{f}\right)^4\right] \quad (1)$$

Where H_S = Significant wave height, f_p = Peak frequency. The attempts have been made to study the effect of system parameters in performance of the device due to random waves. To bring in more clarity over the wave structure interaction the ratio of zeroth spectral moment of front wall outside pressure, front wall inside pressure, air chamber pressure to that of zeroth spectral moment of incident wave are analyzed and presented as a function of d/L_p. In order to understand the hydrodynamic feature of the OWC, wave amplification (β) and power conversion efficiency (λ) inside the air chamber are taken for analysis. The prominent results from the study are discussed below.

3.2 *Front wall outside pressure*

In order to comprehend the wave and structural interaction, the ratio of zeroth spectral moment of front wall outside pressure, $[(m_0)_r]_{fout}$ to that of the incident wave, $(m_0)_\eta$, hereinafter termed as '$[(m_o)_r]_{out}$' is shown in Figure 4, as a function of d/L_p for a range of H_{m0}/d between 0.1010 and 0.1564. It is found that $[(m_o)_r]_{out}$ decreases with an increase in d/L_p since pressures exerted on structures due to long waves are higher. In other words this is just the pressure decay of high frequency components. Further, it is noticed that for d/L_p less than 0.15, $[(m_o)_r]_{out}$ is greater than unity. Although the magnification of pressures is due the reflection of waves from the front wall, the bottom profile of the OWC can also have an effect. As the circular arc bottom profile having the smooth curvature to the entering waves and least reflection compared to other bottom profiles creates minimum pressure setup outside the front lip wall. In a similar way, the slope 1 in 5 also makes smoothened obstruction to the incoming waves resulting in lesser front wall outside pressure. Unlike the OWC with its base being circular arc and slope 1 in 5, the one with a flat bottom does not have the smooth curvature leading to high pressures. The OWC with a bottom slope of 1 in 1, due to maximum reflection exhibits maximum pressure. Thus from the point view of the magnitude of pressures exerted on the front wall, OWC with its base formed by a circular arc would be preferred.

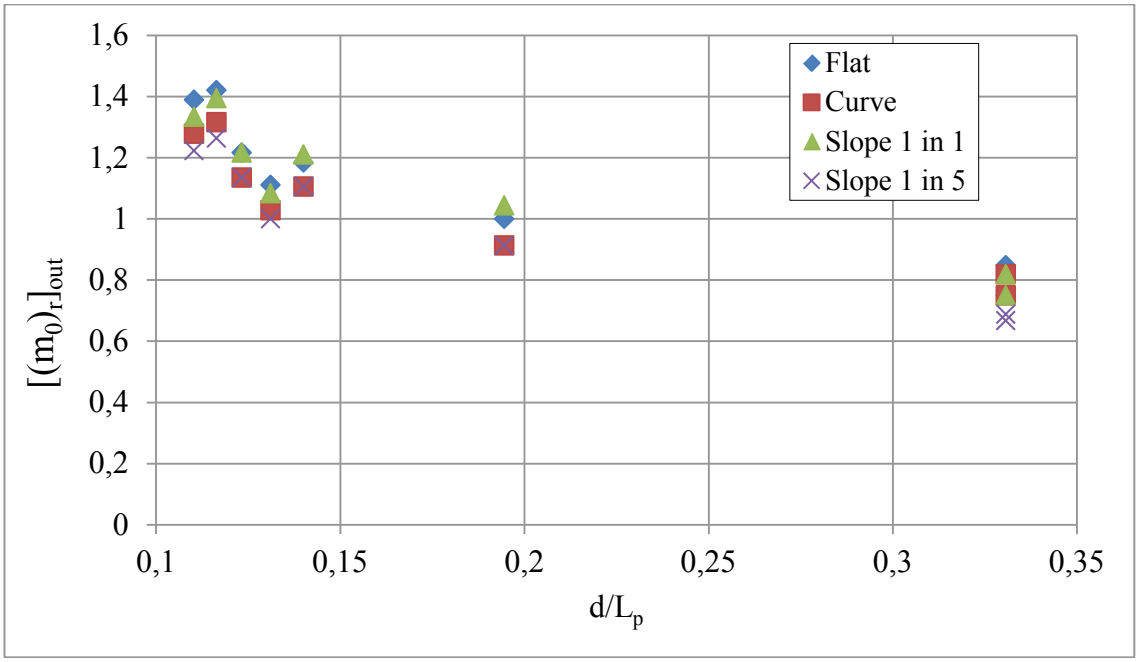

Figure 4. Variation of $[(m_o)_r]_{out}$ with d/L_p (H_{m0}/d from 0.1010 to 0.1564)

3.3 *Front wall inside pressure*

In an OWC, the magnitude of oscillation of air column above the water surface inside the air chamber qualifies the energy conversion capacity of the device. The ratio of zeroth spectral moment of pressure inside the front wall, $[(m_0)_r]_{fin}$ to that of the incident wave, $(m_0)_\eta$, hereinafter termed as '$[(m_o)_r]_{in}$' is shown in the Figure 5, as a function of d/L_p for a small range of H_{m0}/d as mentioned earlier.

In the Figure 5, it is observed that the trend in the variation is found to be similar that of observed for the front wall outside pressure port. A critical look at the variations show a rapid decrease in $[(m_o)_r]_{in}$ by about 40 to 75% for higher frequency wave components, i.e., for $d/L_p > 1.5$. During the passage of low frequency waves, most of the energy in such waves penetrates into the chamber leading to increased pressure on the wall as well as the oscillations of the water surface.

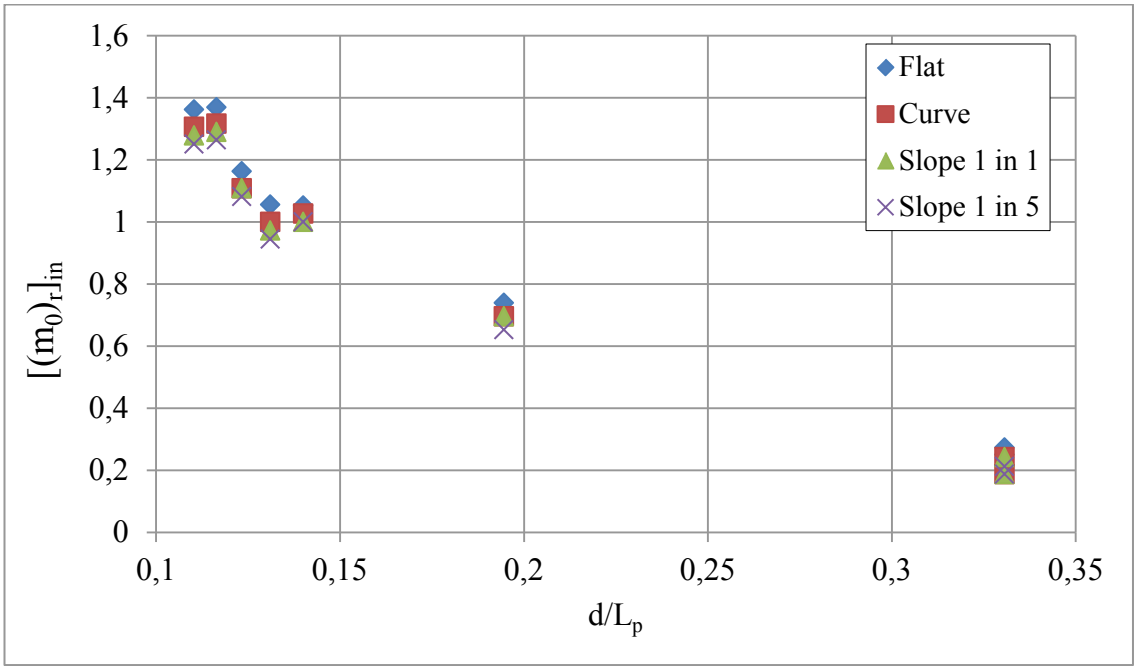

Figure 5. Variation of $[(m_o)_r]_{in}$ with d/L_p (H_{m0}/d from 0.1010 to 0.1564)

3.4 *Air Chamber Pressure*

The air chamber energy conversion process is complex. The exit of air from the chamber and its interaction with the incoming air from outside the OWC causes the pneumatic damping combined with the secondary flow causes a radiated flow inside the air chamber. The ratio of zeroth spectral moment of air pressure, $[(m_0)_r]_a$ to that of the incident wave, $(m_0)_\eta$, hereinafter termed as '$[(m_o)_r]_{air}$' is shown in the Figure 6, as a function of the relative water depth d/L_p with the H_{m0}/d ranges from 0.1010 to 0.1564.

The results indicate the air pressure inside the OWC chamber is about 50% of pressures inside and outside the front wall. Further, for the OWC with curved bottom, $[(m_o)_r]_{air}$ is observed to be almost a constant for the entire range of d/L_p, whereas, for the other configurations, this varies. It is to be mentioned that is important to reduce the random nature of air pressure variation by some process; herein, the adopted percentage of air opening to the plan area is 0.68% which controls the air pressure variation. The steep bottom profile slope 1 in 1 exhibits higher air development. In the case of flat bottom profile, the magnitude of air pressure developed is less due to radiated flow inside the air chamber. The air pressure developed by slope 1 in 5 bottom profile is observed to be closer to that with the circular arc profile which is basically due to larger pressures exerted on the inner wall due to the incident waves. With a minimum variation in the air pressure, the production and transmission and of power could be smooth. Further the strain on the turbine will be a minimum. The above results show that the OWC with a circular arc bottom exhibits a smooth variation in $[(m_o)_r]_{air}$ and hence could be preferred.

3.5 *Wave Amplification Factor*

The phenomena of wave amplification factor of free surface elevation inside the chamber $\beta=(R_u/H_{mo})$ with d/L_p for H_{m0}/d ranging from 0.1010 to 0.1564 are shown in Figure 7. The nature of variation includes the combined effect of radiated flow due to different bottom profile configuration indicates circular arc bottom profile have the higher wave amplification compare to other bottom shapes.

The circular arc bottom profile is a smooth curvature to the passage of the wave results in higher wave amplification. The bottom with flat and slope of 1 in 5 bottom profiles experiences a reduction in the amplification by about 10 to 20% that of the device with curved bottom for the entire range of d/L_p tested. The device with a bottom slope of 1 in 1 is found to experience least wave amplification due to reflection of waves.

The circular arc bottom profile is a smooth curvature to the passage of the wave results in higher wave amplification. The bottom with flat and slope of 1 in 5 bottom profiles experiences a reduction in the amplification by about 10 to 20% that of the device with curved bottom for the entire range of d/L_p tested. The device with a bottom slope of 1 in 1 is found to experience least wave amplification due to reflection of waves.

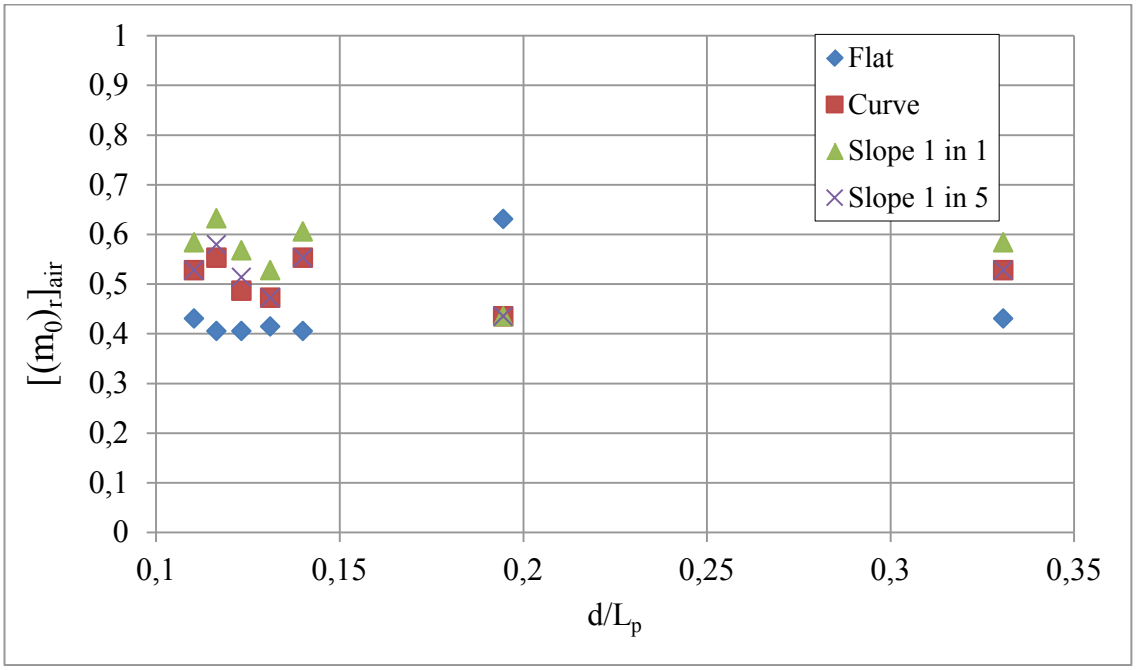

Figure 6. Variation of '$[(m_o)_r]_{air}$ with d/L_p (H_{m0}/d from 0.1010 to 0.1564)

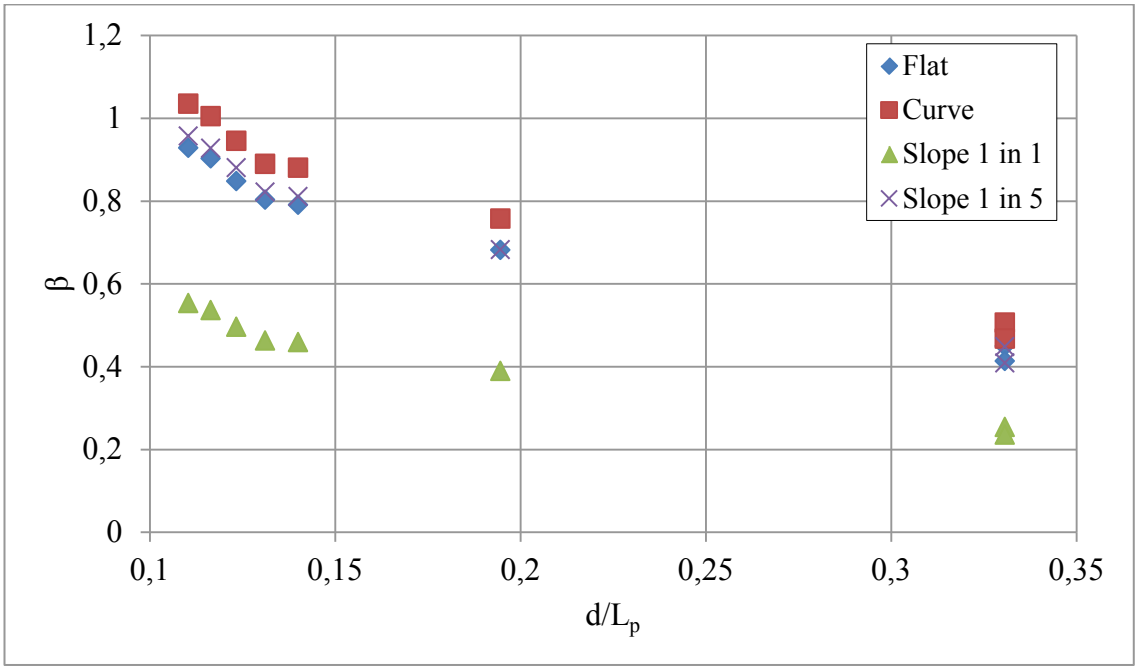

Figure 7. Effect of bottom profile configuration on β with d/L_p (H_{m0}/d from 0.1010 to 0.1564)

The circular arc bottom profile is a smooth curvature to the passage of the wave results in higher wave amplification. The bottom with flat and slope of 1 in 5 bottom profiles experiences a reduction in the amplification by about 10 to 20% that of the device with curved bottom for the entire range of d/L_p tested. The device with a bottom slope of 1 in 1 is found to experience least wave amplification due to reflection of waves.

3.6 *The Hydrodynamic Efficiency of an OWC*

The OWC when exposed to random waves, the air pressure and the velocity of free surface will also be the random. Thus, the device has to be optimized to average power production. The hydrodynamic efficiency of an OWC device is calculated by an expression is given in Equation 2.

$$\lambda = \frac{P_{ave}}{P_{in}} \tag{2}$$

Where, λ= Hydrodynamic efficiency, P_{ave}= average air pressure (at top plate of the chamber) and P_{in} = input power. The average air pressure is calculated by an expression is given in Equation 3.

$$P_{ave} = \frac{1}{2} p_0 A v_0 \tag{3}$$

Where, p_0 = Significant air pressure, A = Plan area of a chamber and v_0= Oscillating velocity of free surface elevation inside the chamber. The input power corresponding to the energy wave period (T_e) calculated by an expression given in Equation 4.

$$P_{in} = \frac{1}{8} \rho g H_{m0}^{\ 2} C_g (T_e, d) W \tag{4}$$

Where, ρ = fluid density, g = gravity acceleration, H_{m0}=Spectral estimate of the significant wave height, C_g = group celerity, d = water depth (0.5m) and W = front opening width of the OWC device (0.471m).

The hydrodynamic efficiency as a function of d/L_p for H_{m0}/d ranging between 0.1010 and 0.1564 is shown in Figure 8.

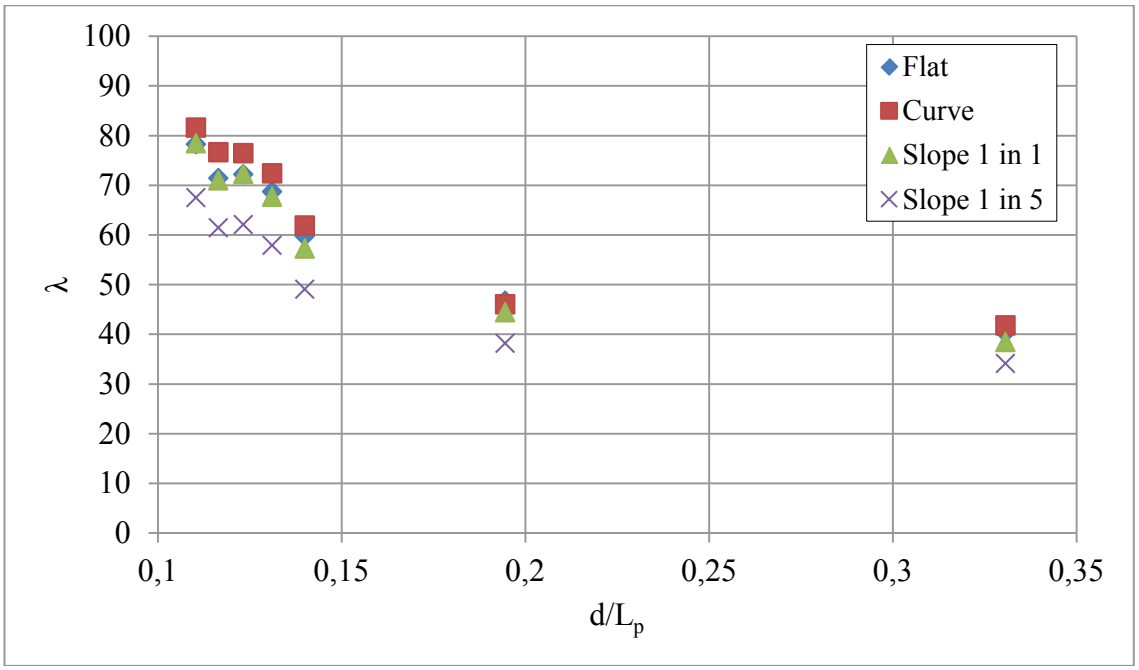

Figure 8. Effect of bottom profile configuration on λ with d/L_p (H_{m0}/d from 0.1010 to 0.1564)

The results show that the hydrodynamic efficiency is observed to be more than 70% for d/L_p less than 0.13 and thereafter, a decrease in the efficiency is clearly noticed. It is also seen that the OWC with circular arc base exhibits maximum efficiency compare to the OWC device with other bottom configurations considered.

4 CONCLUSIONS

An experimental study was performed on a single chamber oscillating water column device model. By comparing the obtained results on the variations in ratio of zeroth spectral moment of front wall outside pressure, front wall inside pressure, air chamber pressure to that of zeroth spectral moment of incident wave, wave amplification and hydrodynamic efficiency, the following conclusions are drawn.

In the lower frequency, '$[(m_o)_r]_{out}$' and '$[(m_o)_r]_{in}$' are to be nearly same, thus, leading to higher efficiency of the system. The $[(m_o)_r]_{out}$ for d/L_p greater than 0.15 is found to be higher than $[(m_o)_r]_{in}$ thus resulting in lesser efficiency.

The air pressure inside the chamber of the OWC with circular arc bottom is mostly centered around the average value for the entire frequency range which is advantageous from power output point of view.

The wave amplification maximum for OWC with circular arc bottom profile because of smooth curvature to the incoming water waves compared to other bottom profiles.

The natural frequency of system is independent of the bottom profile and occurs in the neighborhood of d/L_p around 0.12.

The OWC models are found to be more efficient in absorbing energy from low frequency waves.

NOTATION

d	water depth
d/L_p	relative water depth
H_{m0}/d	depth limited wave breaking criteria
R_u	run up
P_{fout}	pressure transducer register pressure variations on front of the lip wall
P_{fin}	pressure transducer register pressure variations on back of the lip wall
P_{air}	pressure transducer register pressure variations on top of the air chamber
H_{m0}	spectral estimate of significant wave height
L_p	peak wave length
H_S	significant wave height
f_p	peak frequency
$[(m_0)_r]_{fout}$	zeroth spectral moment of front wall outside pressure
$[(m_0)_r]_{fin}$	zeroth spectral moment of front wall inside pressure
$[(m_0)_r]_a$	zeroth spectral moment of air pressure
$[(m_o)_r]_{out}$	ratio of zeroth spectral moment of front wall outside pressure to that of the incident wave
$[(m_o)_r]_{in}$	ratio of zeroth spectral moment of front wall inside pressure to that of the incident wave
$[(m_o)_r]_{air}$	ratio of zeroth spectral moment of front wall air pressure to that of the incident wave
β	wave amplification
λ	hydrodynamic efficiency
P_{ave}	average air pressure
P_{in}	input power
ρ	fluid density
g	gravity acceleration
p_0	significant air pressure
v_0	oscillating velocity of free surface elevation inside the air chamber
T_e	energy wave period
C_g	group celerity

REFERENCES

Evans, D.V., and R. Porter (1995) Hydrodynamic characteristics of an oscillating water column device, Applied Ocean Research, 18, 155-164.

Falnes, J. (2005) Ocean waves and oscillating systems. Cambridge University Press, ISBN 1139431935.

Malmo, O., Reitan, A., 1985. Wave-power absorption by an oscillating water column in a channel. Journal of Fluid Mechanics 158, 153–175

McIver, P., and D.V. Evans (1988) An approximate theory for the performance of a number of wave energy devices set into a reflecting wall. Applied Ocean Research, 10(2), 58-65.

Sundar, V., M. Torgeir, and H. Jorgen (2010) Conceptual Designs on Integration of Oscillating Water column Devices in Breakwaters, Proc of the ASME 29th Intl. Conf. on Ocean, Offshore and Arctic Eng: 2010. 479-489.

Thiruvenkatasamy, K., and S. Neelamani (1997) On the efficiency of wave energy caisson in array. Applied Ocean Research.19, 61-72.

Thomas, M.T.M., R.J. Irvin, and K.P. Thiagarajan (2007) Investigation into the hydrodynamic efficiency of an oscillating water column, J offshore MechArctEng:, 129, 273-80.

Wilbert, R., Sundar,V. and Sannasiraj, S.A. (2013) Wave interaction with double chamber oscillating water column device. International Journal of Ocean and Climate Systems, 4(1).21-39.

Zhang, Y., Q.P. Zou, and D. Greaves (2012) Air-water two phase flow modelling of hydrodynamic performance of an oscillating water column device. Renewable Energy. 2012(41), 159-170.

Zheng, W. (1989) Experimental Research and parameters optimization of a prototype OWC wave power device. Proceedings of the International Conference on Ocean Energy Recovery ‘89, 43-50.